

# We are IntechOpen, the world's leading publisher of Open Access books Built by scientists, for scientists

6,400

Open access books available

174,000

International authors and editors

190M

Downloads

Our authors are among the

154

Countries delivered to

TOP 1%

most cited scientists

12.2%

Contributors from top 500 universities



WEB OF SCIENCE™

Selection of our books indexed in the Book Citation Index  
in Web of Science™ Core Collection (BKCI)

Interested in publishing with us?  
Contact [book.department@intechopen.com](mailto:book.department@intechopen.com)

Numbers displayed above are based on latest data collected.  
For more information visit [www.intechopen.com](http://www.intechopen.com)



## Chapter

# Artificial Intelligence Approaches for Studying the $pp$ Interactions at High Energy Using Adaptive Neuro-Fuzzy Interface System

*Doaa Mahmoud Habashy, Mahmoud Yaseen El-Bakry, El-Sayed Ahmed El-Dahshan and Hanem Ibrahim Lebda*

## Abstract

Adaptive Neuro-Fuzzy Inference System (ANFIS), a popular machine learning model, is introduced in this chapter. ANFIS has a long development history and good agreement on scientific accomplishments. The value of ANFIS has grown dramatically along with the great interest in deep learning. We will examine how machine learning and ANFIS are related. Different methods can be used to implement machine learning models. ANFIS is a Fuzzy Inference System (FIS) that works within the context of adaptive networks. It merges the ideas of Artificial Neural Networks (ANNs) and Fuzzy Logic (FL) into a single framework. This framework can learn to estimate nonlinear functions and operates as a universal estimator. This chapter aimed to investigate the behavior of  $D$  mesons ratios production cross section ( $D^+/D^0, D^{*+}/D^0, D_s^+/D^0$ , and  $D_s^+/D^+$ ), differential production cross section of prompt ( $D^0, D^+, D^{*+}$  and  $D_s^+$  mesons) as a function of  $P_T$  in  $pp$  collisions at ( $\sqrt{s} = 5.02$  and  $7$  TeV) and predict the behavior for others. The ANFIS model was created through a series of trial-and-error experiments. The ANFIS-based model simulation results perfectly fit the experimental data. When tested with non-training data points, the ANFIS prediction capabilities performed well. The ANFIS offers extensive procedures for high-energy physics modeling.

**Keywords:** adaptive neuro-fuzzy interface system, artificial neural network, deep learning, machine learning, artificial intelligence

## 1. Introduction

Artificial Intelligence (AI) has been quickly assimilated into our daily lives during the past 10 years. It drives a lot of our behaviors, including how we use social media and definitely the future of the planet. So to be employable in the expanding sector, it is essential to understand the primary distinctions between Artificial Intelligence (AI), Machine Learning (ML,) and Deep Learning (DL) [1–5]. We will define AI, ML, and

DL in the following sections, as well as emphasize the key distinctions between the two latter subsets (see **Figure 1**).

The term “Artificial Intelligence” was popularized in 1956 at the Dartmouth conference, which was organized by John McCarthy, the father of AI. It is the development of intelligent devices and systems that are capable of performing tasks which would normally require human intelligence. It is defined as a branch of computer science concerned with the simulation of intelligent behaviors in computers. AI systems possess the ability to do a variety of activities similar to human intellect, including planning, learning, manipulation, and problem-solving. Artificial narrow intelligence and artificial general intelligence are the two most commonly types of artificial intelligence. Narrow Artificial Intelligence is systems or computers with artificial limited intelligence, commonly referred to as weak AI, that are capable of carrying out solitary tasks. However, they are unable to perform tasks that are not part of their intended function and capability. The kinds of AI machines or programs that we use on a daily basis are instances of limited or weak AI. Examples that are often used include facial recognition software, email spam filters, and Google Translate. General Artificial Intelligence is a more sophisticated machine that has all of a human’s talents, including emotional intelligence and creativity, which is referred to as strong AI. However, it is a difficult challenge that has not yet succeeded in replicating human intelligence, emotions, and the capacity to respond in unanticipated circumstances. The only way we can see this type of AI in action is in science fiction films. Machine Learning (ML) is a branch of AI [6]. It focuses on developing algorithms that can take in the provided data, learn from it, and make judgments based on the patterns found in it. When an unpleasant or wrong choice is made, these intelligent systems will need human intervention. ML is used to teach machines how to manage data more efficiently. We may be unable to perceive the obtained information from the data after viewing it. In that case, we employ ML. With an abundance of datasets available, the demand for machine learning is increasing. Many industries use ML to extract data. The goal of ML is to learn from data. Deep Learning (DL) is a further division of ML. Without requiring human input, it processes data using a number of layers of algorithms and artificial neural network to arrive at an accurate conclusion. DL was first introduced in the 1980s, but it has achieved popular success since 2006. Due to the enormous quantity of data needed to train a DL network, significant computational power and time are required. The time required to train the network could eventually be cut in half, from weeks to hours, as cloud computing and Graphics Processing Units

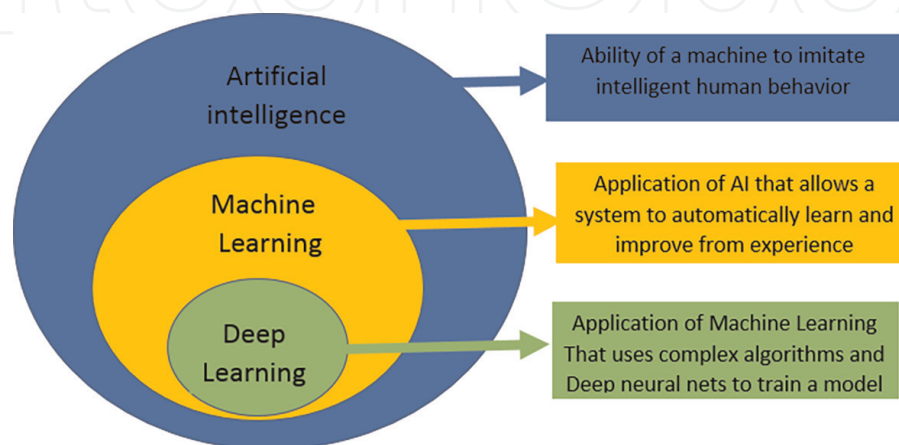


**Figure 1.** Overview of artificial intelligence (AI), machine learning (ML) and deep learning (DL).

(GPUs) advance and grow. As shown in **Table 1**, there are some significant differences between DL and ML based on the descriptions of both concepts above [7–10].

A component of AI called ML, teaches programs how to spot patterns in datasets and use those patterns to infer conclusions and predictions. The use of datasets, features, and algorithms in ML software is essential. Datasets are used to train machine learning programs to identify patterns and correlations, so they are necessary. Images, numbers, words, and other types of data are included in such databases. Features, often known as variables, draw attention to important data points that the program should concentrate on. In order to teach the program how to make the best judgments, the appropriate features and algorithms must be chosen. These features and algorithms are the tools for data analysis. The speed and precision of getting the results may vary, even when utilizing multiple methods for the same task may produce equal solutions. It's also crucial to remember that the accuracy of the results is determined by the caliber of the data. Therefore, gathering reliable data will help in reaching the intended results [11, 12].

Forecasting and prediction of data, such as stock market prices, are frequent applications of machine learning. Other straightforward applications that employ it include email spam filters and social media connection suggestions. While DL is used in more complex situations like autonomous vehicles. The network is able to identify traffic lights, find barriers, and more. AI approaches have been recently used in a number of modeling methodologies based on soft computing systems. In the fields of nuclear physics, high-energy physics, materials science, and other sciences, these evolution algorithms have a strong physical existence. The Interaction behavior is complicated by the non-linear relationship between the interaction parameters and the result. AI approaches are essential for the multi-part data processing required to understand the interactions of fundamental particles. These techniques act as alternatives to more traditional methods. In this regard, AI methods like genetic algorithms, genetic programming, and Genetic Expression Programming (GEP) can be used as substitute tools to imitate these interactions. The learning algorithm of AI approaches serves as a driving force behind their use, as it discovers the links between variables in datasets. Then builds models to account for those associations (mathematically dependent). To evaluate experimental data and gain a better knowledge of many physics processes, a new computer science approaches are needed. Experimental data were acquired and described by a mathematical equation.

The success of modeling enables us to anticipate areas where experimental data are lacking. Due to its generalization, noise tolerance, and fault tolerance, AI has become increasingly popular in recent years as a potent tool for creating data correlations and

	<b>Machine learning (ML)</b>	<b>Deep learning (DL)</b>
Approach	Requires structured data	Does not require structured data
Human Involvement	Requires human Involvement for mistakes	Does not require human Involvement for mistakes
Hardware	Can function on CPU	Requires GPU/ significant computing power
Time	Takes seconds to hours	Takes weeks
Uses	Forecasting, predicting, and other simple applications	More complex applications like autonomous vehicles

**Table 1.**  
 Comparison between DL and ML.

has been successfully applied in materials science. Alaa F. Abd El-Rehim et al., used ANN to Simulate and forecast the Vickers Hardness [13–16]. H A M Ali and D M Habashy used ANN model for calculating the electrical impedance, AC conductivity and dielectric properties [17]. D. M. Habashy et al., simulate and forecast Entropy per Rapidity using ANN model at LHC Energies [18]. D. M. Habashy et al., used ANN model for training Particles multiplicity per rapidity for different charged particles observed in Au + Au heavy-ion collisions with energies varying between 2 and 200 GeV [19]. D.M. Habashy et al., train and forecast micro-hardness of nano-crystalline TiO<sub>2</sub> using ANNs [20].

## **2. Applications in industry**

Our GPS navigation systems' traffic predictions are made using machine learning algorithms [1–3]. Based on location- and velocity-related data acquired from our daily data feedback, they indicate busy routes. In order to suggest people we might know, ML software analyze our social media usage data, including the people we have connected with, the profiles we have visited, and our hobbies. Email spam filters use ML to deliver a more dependable and resilient solution. It guarantees that the filter is continually updated to recognize the most recent spammers' tricks. The AlphaGo program from Google DeepMind is among the most well-known applications of deep learning. Go is a board game that the system learned to play by competing against expert players. By making plays without the aid of a human, it was finally able to play at a level above that of the world champion Lee Sedol. One business adopting deep learning for self-driving cars is Tesla. Their deep learning program is utilized for semantic segmentation, road item detection and avoidance, monocular depth estimation, and image analysis. Amazon developed Alexa Conversations to give people a more organic engagement experience. Deep learning is used to ensure more natural interactions rather than ones that are forced or inflexible. On the basis of the presented photos, a deep learning (DL) system is asked to distinguish between dogs and cats. These photos will first be sent via the neural network's various levels. The subsequent layers will individually identify the distinctive features of dogs and cats, ultimately establishing the proper characteristics of each species. Finally, it will generate a result that accurately separates the photos into those of dogs and cats. Unlike the preceding machine learning example, the deep learning system in this case does not need structured data to categories the animals.

## **3. Artificial neural networks (ANNs) and their constituent parts**

Data inputs, weights, biases, activation functions, and outputs make up ANNs [4, 13, 21].

1. These are the data that you wish to process, or data inputs.
2. Weights: These specify how significant each input is to the final result.
3. Biases: These reflect the degree to which assumptions about the outcome are made. More Inferences are made when the bias is larger, while less Inferences are made when the prejudice is smaller.

4. The weighted average of the inputs and the bias used make up the activation functions. They make the decision on whether or not the data will move on to the network's next layer.

Artificial neurons are present in every layer of a NN and transmit data through them. There is bias in these neurons. Weighted channels are used to convey inputted data via the layers. The weighted value of the data is added to the bias and used within the activation mechanism when it reaches the neurons. The neuron may or may not be triggered according to the outcome of the function. If the neuron is active, the information will be transmitted to the following layer. The data will not move on to the next layer, though, if it's not active. Until an output is created, this process will be repeated across the layers. Decisions produced by the deep learning software are the outputs. DL system does not require human involvement to learn from their mistakes because of the various layers in the neural network. It represents a meager step toward creating an artificial general intelligence system that is capable of autonomous decision-making.

#### 4. Adaptive neuro-fuzzy inference system (ANFIS)

As is well known, the fuzzy logic system has some limitations, such as the need to determine the rule base, which is usually solved by referring to expert knowledge. It is obvious that the membership functions required for the formation of fuzzy sets must be determined. ANFIS allows you to use data sets to determine the rule base and membership functions for this purpose [22–25]. The ANFIS system employs two approaches: NNs and FL, if these two systems are merged, they may obtain a successful outcome that involves either fuzzy intelligence or neural network analytical abilities. The ANFIS structure, like that of other fuzzy systems, is divided into two parts: introductory and concluding, which have been connected by a set of rules. ANFIS training includes determining the parameters associated with these parts and using an optimization algorithm. During training, ANFIS makes use of the existing input–output data pairs. And after that, IF-THEN fuzzy rules are created to determine how these parts are related to one another (Jang 1993).

##### 4.1 ANFIS architecture

ANFIS structure is formed of nodes and the bonds that link them. Because some or all of the nodes have influence over the end nodes, it is adaptive. An algorithm is applied to discover the relationship between input and output nodes. We can see 5 different layers in the ANFIS network structure, denoting that it is a multi-layer network. The structure has 2 inputs and one output, as well as four membership functions and two rules. The layer structure of ANFIS is explained below in accordance with the ANFIS structure shown in **Figure 2**.

The input values are obtained by the first layer, which defines the membership functions that apply to them. The “fuzzification layer” is also called. This layer's outputs are the inputs' fuzzy membership grades, which are determined using the following equations:

$$O_{1,i} = \mu_{A_i}(x), i = 1, 2 \quad (1)$$

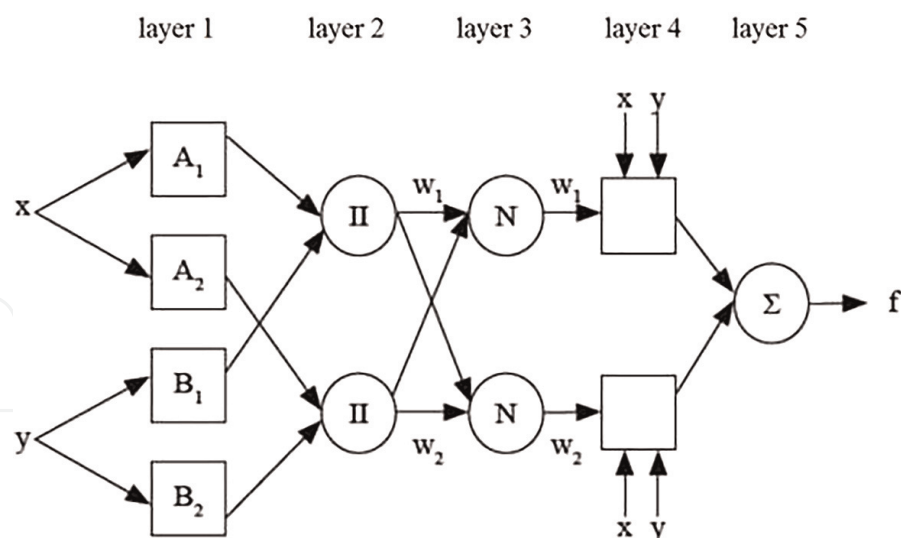


**Figure 2.**  
ANFIS general structure in five layers.

$$O_{1,i} = \mu_{B_i}(y), i = 3, 4 \quad (2)$$

Where  $x$  and  $y$  are the node's inputs, and  $A_i$  and  $B_i$  are the verbal marks linked with this node function.  $\mu_{A_i}(x)$  and  $\mu_{B_i}(y)$  can be assigned any fuzzy membership function. Due to function, the 2nd layer is called the rule layer because it multiplies the input signal values into each node and determines the rule firing strength. This layer employs fuzzy operators to fuzzify the inputs, and also the AND operator. The output of the 2nd Layer is as follows:

$$O_{2,i} = \omega_i = \mu_{A_i}(x) * \mu_{B_i}(y), i = 1, 2 \quad (3)$$

The third layer's role is to normalize the computed firing strengths by dividing each value by the total firing strength, and it is referred to as the normalization layer, the output of Layer 3  $\bar{\omega}_i$  is as follows:

$$O_{3,i} = \bar{\omega}_i = \frac{\omega_i}{\omega_1 + \omega_2}, i = 1, 2 \quad (4)$$

The fourth layer will receive the normalized input values combined with the result parameter set and is called as defuzzification layer.

$$O_{4,i} = \bar{\omega}_i f_i = \bar{\omega}_i (p_i x + q_i y + r_i), i = 1, 2 \quad (5)$$

Where  $p_i, q_i,$  and  $r_i$  are the consequent parameters.

In the network's final layer, a single fixed node labeled ANFIS calculates the total output as the cumulative of all input variables. The model's overall output is given by

$$O_{5,i} = \sum_i \bar{\omega}_i f_i = \frac{\sum_i \omega_i f_i}{\sum_i \omega_i}, i = 1, 2 \quad (6)$$

During the training process, the best values of MF such as (Triangular.—Trapezoidal.—Piecewise linear.—Gaussian.—Singleton) and subsequent parameters for

ANFIS model experiences are noted as a training data set and training algorithms, see **Figure 3**. The ANFIS model was trained to utilize backpropagation and hybrid algorithms. The backpropagation algorithm calculates output errors for each layer and uses them to update layer parameters. The hybrid training algorithm is so named because it employs two gradient descent and least-squares optimization techniques.

ANFIS was created using MATLAB software, and various membership functions were used to train it. To achieve the optimal membership function parameters, the ANFIS approach's inputs are fuzzified with membership functions and trained using training data measured under normal and abnormal conditions.

#### 4.2 The proposed hybrid ANFIS modeling

The present work proposed a hybrid model combined of ANN and FL (called ANFIS model). This model optimize  $D$  mesons ratios production cross-section ( $D^+/D^0, D^{*+}/D^0, D_s^+/D^0$  and  $D_s^+/D^+$ ) and differential production cross section of prompt  $D^0, D^+, D^{*+}, D_s^+$  mesons as a function of Transverse momentum distribution ( $P_T$ ) in pp. collisions at different the total center of mass energy,  $\sqrt{s} = 5.02$  and 7 TeV [26, 27]. Eight ANFIS models are designed to achieve this goal using MATLAB ANFIS editor. ANFIS (1–4) models simulate and predict Ratios of  $D$ —meson  $D^+/D^0, D^{*+}/D^0, D_s^+/D^0$  and  $D_s^+/D^+$  respectively. The inputs of these models are Transverse momentum distribution ( $P_T$ ) and  $\sqrt{s}$ , while the output is Ratios of  $D$ —meson. ANFIS (5–8) models simulate differential production cross section of prompt  $D^0, D^+, D^{*+}, D_s^+$  mesons respectively. The inputs of these models are Transverse momentum distribution ( $P_T$ ) and  $\sqrt{s}$ , while the output is differential production cross section of prompt  $D^0, D^+, D^{*+}, D_s^+$  mesons. The data collected from experiments are divided into two sets, namely, training set and testing set. The training set is used to train the ANFIS hybrid model. The testing data set is used to confirm the accuracy of the proposed model. It ensures that the relationship between inputs and outputs, based on the training and test sets are real. The data set is divided into two groups, 70% for training and 30% for testing. As a neural network, ANFIS must also be taught over a predetermined number of training cycles (epochs). **Figure 4** displays a flowchart of the ANFIS. To determine the ideal architecture parameters, the ANFIS model was run using experimental data. Different training epoch counts were used in several simulations to test how closely the check error (the difference between the output of the ANFIS and the validation data) and training error (the difference between the output of the ANFIS and the training data) were

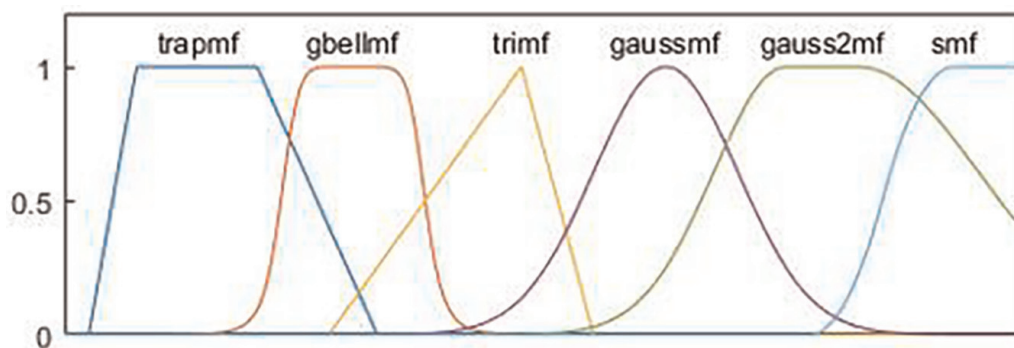


**Figure 3.**  
Membership functions.



related (so that ANFIS would have generalization capability). The root mean squared error (RMSE) and coefficient of correlation ( $R^2$ ), both of which are provided in Eqs. (7) and (8) respectively, are statistical measures that are used to evaluate error.

$$RMSE = \sqrt{\frac{\sum_{i=1}^n (Opre_i - Oexp_i)^2}{n}} \quad (7)$$

$$R^2 = 1 - \left( \frac{\sum_i (Opre_i - Oexp_i)^2}{\sum_i (Opre_i)^2} \right) \quad (8)$$

The predicted and experimental outputs are represented by  $Opre_i$  and  $Oexp_i$ , respectively, and  $n$  is the number of paired input/output pairs.

## 5. Results and discussion

The goals of this chapter are to use the ANFIS model to model, simulate and predict the behavior of  $D$  mesons ratios production cross-section ( $D^+/D^0, D^{*+}/D^0, D_s^+/D^0$  and  $D_s^+/D^+$ ) and differential production cross section of prompt ( $D^0, D^+, D^{*+}$  and  $D_s^+$  mesons) as a function of  $P_T$  in pp. collisions at ( $\sqrt{s} = 5.02$  and 7 TeV).

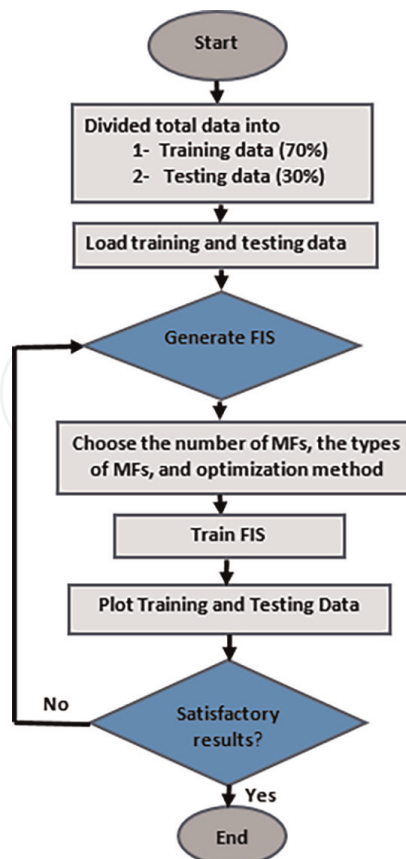


**Figure 4.** Flowchart of ANFIS model.

Specific steps are taken in order to achieve the chapter's objectives. The ANFIS model is loaded with experimental data. MATLAB is utilized to process the modeling (R2017 a). Eight ANFIS networks have been generated to finish the modeling process for  $D$  mesons ratios production cross-section ( $D^+/D^0, D^{*+}/D^0, D_s^+/D^0$  and  $D_s^+/D^+$ ) and differential production cross section of prompt ( $D^0, D^+, D^{*+}$  and  $D_s^+$  mesons) as a function of  $P_T$  in pp. collisions at ( $\sqrt{s} = 5.02$  and 7 TeV). For each ANFIS network, the number and the type of membership functions (MF) for both inputs and outputs are determined. The number of epochs is also adjustable to obtain the lowest training error. After re-training multiple ANFIS networks with various specifications, the optimal ANFIS network with the lowest possible training error is discovered. The input patterns of the designed ANFIS hybrid have been trained to produce target patterns that modeling  $D$  mesons ratios ( $D^+/D^0, D^{*+}/D^0, D_s^+/D^0$  and  $D_s^+/D^+$ ) and differential production cross section of prompt ( $D^0, D^+, D^{*+}, D_s^+$  mesons) as a function of  $P_T$  in pp. collisions at ( $\sqrt{s} = 5.02$  and 7 TeV).

The best ANFIS network for this dataset was found within 50 epochs and two hidden layers with 6 and 6 neurons as specified in **Figure 5**. Membership functions (MFs) also play a fundamental role in Fuzzy Inference Systems modeling. It is worth mentioning that these system modeling are chosen carefully. The performance of ANFIS is very sensitive to the amount of MFs in the system. As a result, it is expected that complex systems with a great quantity of MFs will perform poorly because of the amount of the premise parameters that need to be estimated. MFs can have many shapes. Accordingly, the results of the experiments show that ANFIS with Generalized bell-shaped (gbellmf) has attained the best performance in all simulated and predicted experimental data (see **Figure 6**). The generalized bell-shaped MF (gbellmf) has a

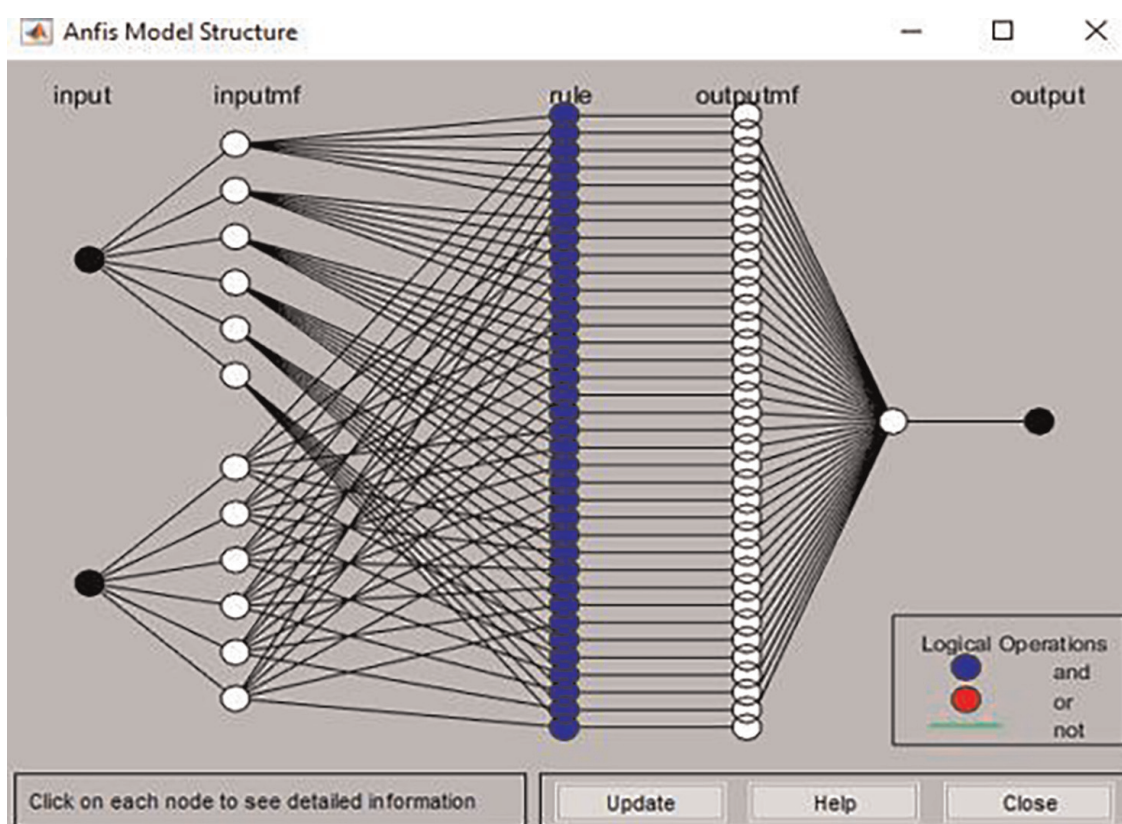


**Figure 5.**  
The ANFIS architecture of the best network.

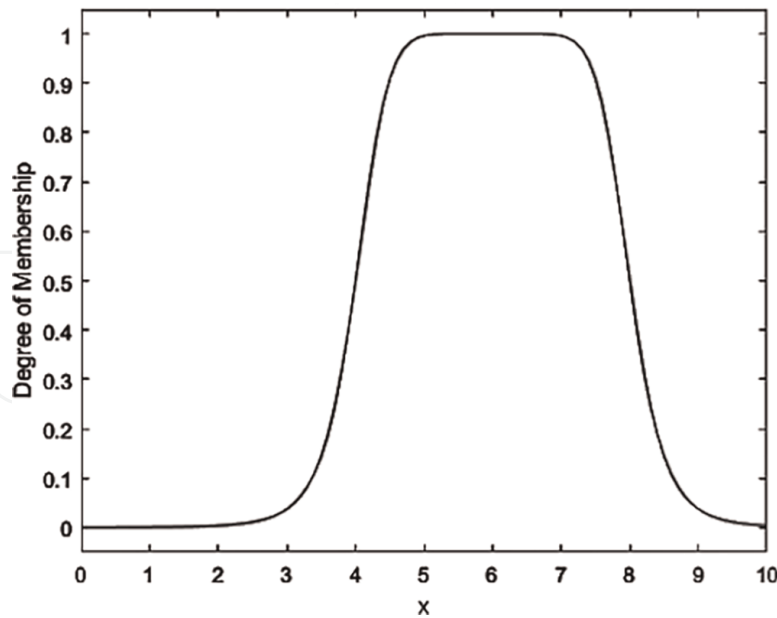


**Figure 6.**  
The generalized bell-shaped membership function (gbellmf).

bell-like symmetrical shape. According to:  $f = (x, a, b, c) = \frac{1}{1 + |\frac{x-c}{a}|^{2b}}$ . This function has three parameters:  $a$  determines the width of the bell-shaped curve, with a larger value resulting in a wider membership function,  $b$  is a positive integer that defines the shape of the curve on either side of the central plateau, and  $c$  determines the center of the curve in a universe of discourse. The function is used to generate an initial output FIS matrix from training data, with default values for membership function numbers “6 6” and types “These defaults” provide membership functions on each of the two inputs. The generated fuzzy inference system structure has 36 fuzzy rules of type “linear” by default. The following are the final parameters that best fit the data.

**ANFIS info.**

Number of nodes: 101

Number of linear parameters: 108

Number of nonlinear parameters: 36

Total number of parameters: 144.

Number of fuzzy rules: 36

Simulation and prediction results based on ANFIS used to model the  $D$ —meson ratios production cross section ( $D^+/D^0, D^{*+}/D^0, D_s^+/D^0$  and  $D_s^+/D^+$ ) and differential production cross section of prompt ( $D^0, D^+, D^{*+}, D_s^+$  mesons) for pp. collision at different  $P_T$  and  $\sqrt{s}$  (5.02 and 7 TeV) are given in **Figures 7–10** (a-d). The experimental data is represented by solid circle symbols, while the simulated ANFIS results are represented by solid line curves and the predicted ANFIS results are represented by solid square symbols. After training, the ANFIS models have been used to predict  $D$  meson ratios at different values of  $P_T$  and  $\sqrt{s}$  (5.02 and 7 TeV) that are not used in training session as shown in **Figures 7–10** (a-d). **Figures 7** and **8** (a-d), they introduce the ANFIS trained results for Transverse momentum distribution measured at  $\sqrt{s}$  (5.02 and 7 TeV) respectively for particles ratios and prediction for experimentally unmeasured values. Studying **Figures 7** and **8**, it was discovered that the simulation ANFIS curves and the experimental data symbols nearly matched, indicating excellent simulation results and the prediction data symbols are clear and produce acceptable

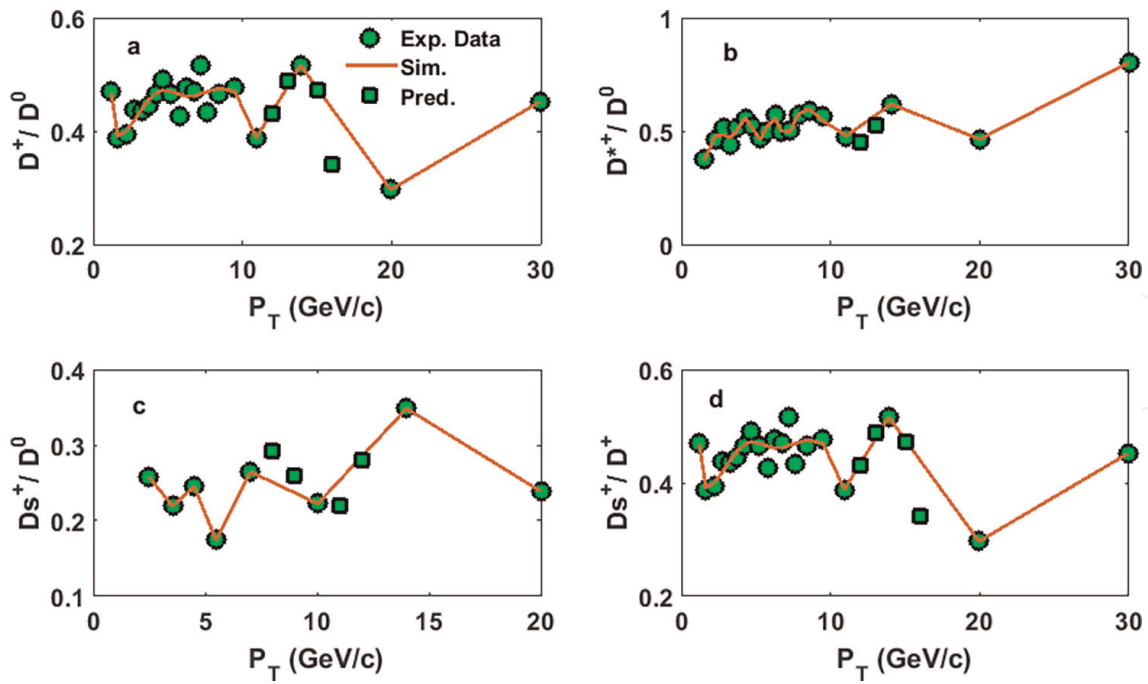


**Figure 7.** Transverse momentum distribution measured at  $\sqrt{s}=5.02$  TeV for particles ratios ( $D^+/D^0$ (a),  $D^{*+}/D^0$ (b),  $D_s^+/D^0$ (c) and  $D_s^+/D^+$ (d) are compared with ANFIS simulation and prediction.

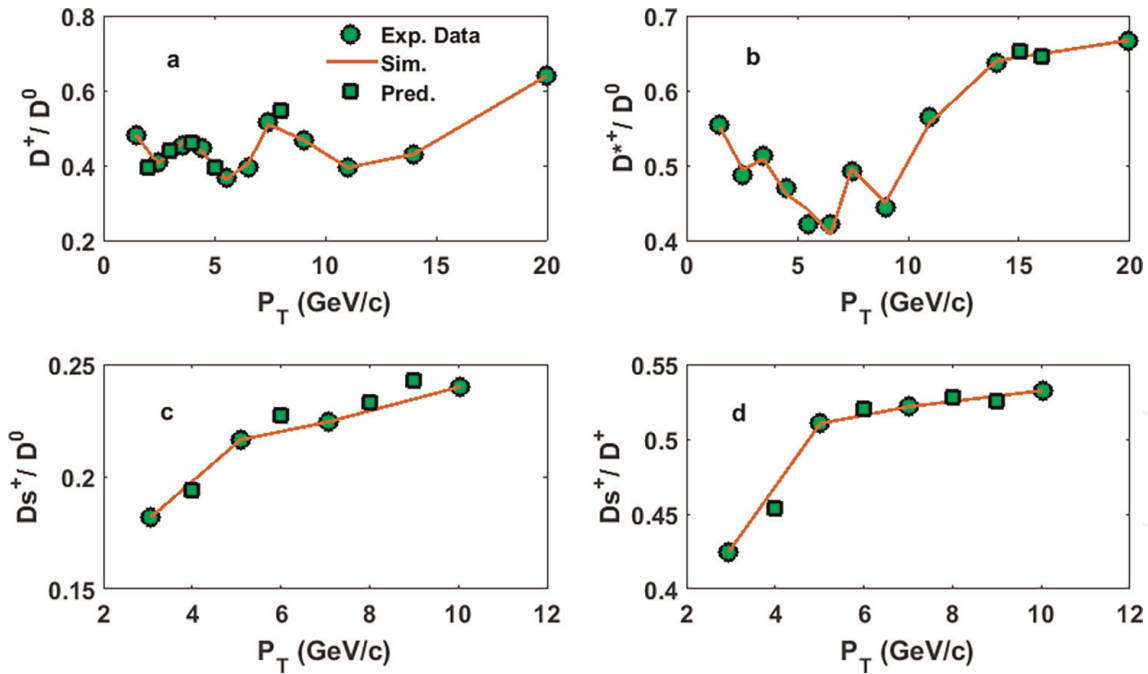


**Figure 8.** Same as in Figure 7 but at  $\sqrt{s} = 7$  TeV.

results. The ratios of the  $P_T$ -differential cross sections of prompt mesons in pp. collisions at  $\sqrt{s} = 5.02$  TeV, the transverse momentum interval  $0 < P_T < 30$  GeV/c are reported in **Figure 7** (a, b, d), and  $0 < P_T < 20$  in **Figure 7**(c) but in **Figure 8** at  $\sqrt{s} = 7$  TeV, the transverse momentum interval  $1 < P_T < 20$  GeV/c are reported in **Figure 8** (a, b), and  $3 < P_T < 12$  GeV/c in **Figure 8** (c, d). In **Figure 9**, the production cross sections were

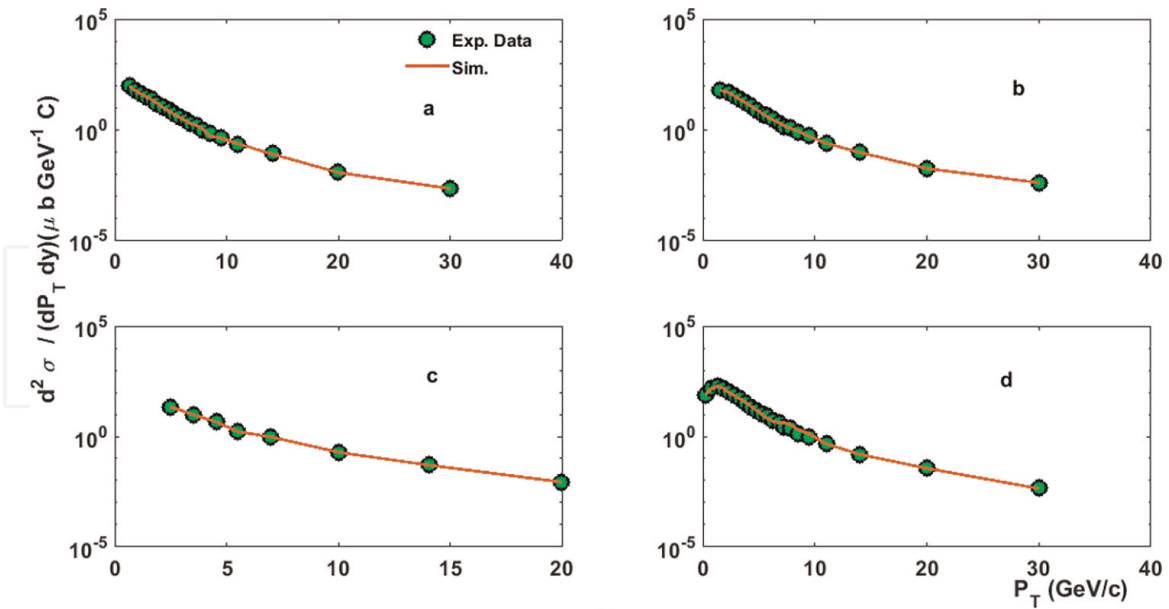


**Figure 9.**  
 $P_T$  differential production cross section of prompt  $D^0$  (a),  $D^+$  (b),  $D_s^+$  (c),  $D^{*+}$  (d) mesons in pp collisions at  $\sqrt{s} = 5.02$  TeV using ANFIS.

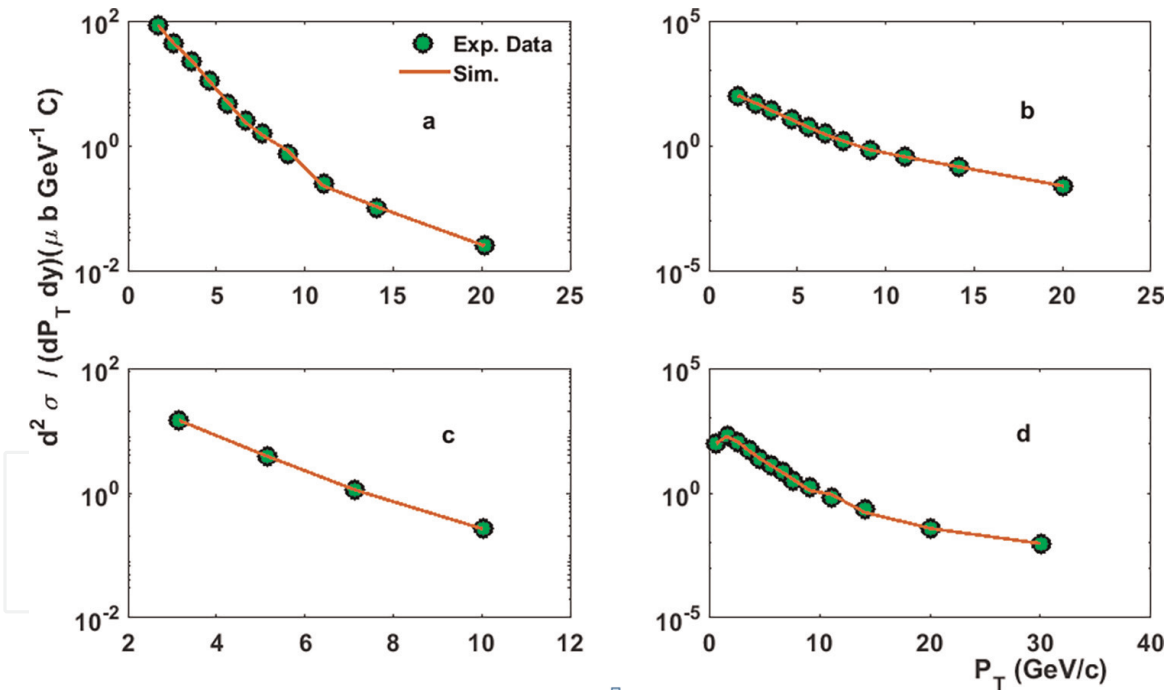


**Figure 10.**  
 Same as in Figure 9 but at  $\sqrt{s} = 7$  TeV.

measured at  $\sqrt{s} = 5.02$  TeV in the transverse momentum interval  $0 < P_T < 30$  GeV/c for  $D^0$ ,  $1 < P_T < 30$  GeV/c for  $D^+$  and  $D^{*+}$ , and in  $2 < P_T < 24$  GeV/c for  $D_s^+$  mesons and were measured at  $\sqrt{s} = 7$  TeV, in the transverse momentum interval  $0 < P_T < 30$  GeV/c for  $D^0$ ,  $1 < P_T < 24$  GeV/c for  $D^+$  and  $D^{*+}$ , and in  $2 < P_T < 12$  GeV/c for  $D_s^+$  mesons as shown in Figure 10. Figures 9 and 10 (a–d), they introduce the ANFIS trained results for  $P_T$  differential production cross section of prompt mesons in pp. collisions at  $\sqrt{s}$  (5.02 and 7 TeV) respectively. The ANFIS simulation results show a high level of

ANFIS parameters type	ANFIS 1 $D^+/D^0$	ANFIS 2 $D^{*+}/D^0$	ANFIS 3 $D_s^+/D^0$	ANFIS 4 $D_s^+/D^+$
$R^2$	0.9327	0.9795	1	1
RMSE	0.151	0.012	$2.07 \times 10^{-7}$	$4.95 \times 10^{-7}$

**Table 2**  
 RMSE and  $R^2$  for  $D$ - meson ratios ( $D^+/D^0, D^{*+}/D^0, D_s^+/D^0$  and  $D_s^+/D^+$ ) in pp collision.

ANFIS parameters type	ANFIS 5 $D^0$	ANFIS 6 $D^+$	ANFIS 7 $D^{*+}$	ANFIS 8 $D_s^+$
$R^2$	0.998	0.999	1	1
RMSE	1.0819	0.2626	0.1426	$1.86 \times 10^{-5}$

**Table 3**  
 RMSE and  $R^2$  for differential production cross section of prompt  $D^0, D^+, D^{*+}, D_s^+$  mesons in pp collision.

agreement with the experimental data. We notice that the curves obtained by ANFIS hybrid model show the best fitting to the experimental data for simulation and prediction. This is agreed with Khajeh [28]; and Tortum, Yayla [29]; and G. M. Behery [30]. The Minimum root mean squared error ( $0.151, 0.012, 2.07 \times 10^{-7}, 4.95 \times 10^{-7}, 1.0819, 0.2626, 0.1426$  and  $1.86 \times 10^{-5}$ ) and higher coefficient of correlation ( $0.9327, 0.9795, 1, 1, 0.998, 0.999, 1$  and  $1$ ) for ANFIS (1–8) respectively were obtained as shown in **Tables 2** and **3** respectively.

## 6. Conclusion

In the area of theoretical high-energy physics, the suggested ANFIS system has gained a good reputation. Due to variations in the kind, quantity, and number of membership functions as well as the number of epochs, the system is intended to identify the best ANFIS that can do the best test and prediction. As a result, numerous efforts are performed to identify the best ANFIS that makes use of a few epochs and membership functions. On the pp. interaction, ANFIS was used and put to the test. The pp. -based ANFIS model calculates  $D$  mesons ratios ( $D^+/D^0, D^{*+}/D^0, D_s^+/D^0$  and  $D_s^+/D^+$ ) and differential production cross section of prompt  $D^0, D^+, D^{*+}, D_s^+$  mesons as a function of  $P_T$  at  $\sqrt{s} = 5.02$  and  $7$  TeV. ANFIS system reached the optimal solution using 50 epochs and 'gbellmf' membership function. The training simulation results demonstrated flawless fitting to the experimental data. With data points not used in training, the ANFIS's prediction ability is tested, and it performs well. The outcomes convincingly show the viability and efficacy of such a method for obtaining collision information. The proposed ANFIS is a powerful mechanism for forecasting the behavior of pp. interaction.

## Acknowledgements

The authors are grateful to Artificial Intelligence Group- Ain Shams University, for it fruitful discussions.

## **Conflict of interest**

The authors declare that they have no conflicts of interest regarding the publication of this chapter.

## **Notes/thanks/other declarations**

The authors would like to thank anonymous for their insightful comments and suggestions for improving the chapter.

## **Author details**

Doaa Mahmoud Habashy<sup>1\*</sup>, Mahmoud Yaseen El-Bakry<sup>1</sup>,  
El-Sayed Ahmed El-Dahshan<sup>2</sup> and Hanem Ibrahim Lebda<sup>1</sup>


1 Faculty of Education, Department of Physics, Artificial Intelligence Group- Ain Shams University, Cairo, Egypt

2 Faculty of Science, Department of Physics, Artificial Intelligence Group- Ain Shams University, Cairo, Egypt

\*Address all correspondence to: [doaamahmoud@edu.asu.edu.eg](mailto:doaamahmoud@edu.asu.edu.eg)

## **IntechOpen**

---

© 2023 The Author(s). Licensee IntechOpen. This chapter is distributed under the terms of the Creative Commons Attribution License (<http://creativecommons.org/licenses/by/3.0>), which permits unrestricted use, distribution, and reproduction in any medium, provided the original work is properly cited. 

## References

- [1] Haykin S. *Neural Networks and Learning Machines*. 3rd ed. Prentice Hall, Upper Saddle River: Pearson; 2008
- [2] Ali-A, Fathalla-A, Salah-A, Bekhit-M, Eldesouky-E. Marine Data Prediction: An Evaluation of Machine Learning, Deep Learning, and Statistical Predictive Models, Computational Intelligence and Neuroscience. 2021;2021:8551167. DOI: 10.1155/2021/8551167
- [3] Kim P. Matlab deep learning With machine learning, neural networks, and artificial intelligence, In *MATLAB Deep Learning*. Apress; 2017. DOI: 10.1007/978-1-4842-2845-6
- [4] Website: <https://www.simplilearn.com/tutorials/artificial-intelligence-tutorial/ai-vs-machine-learning-vs-deep-learning> [Accessed: December 10, 2022].
- [5] EL-Sayed AE, El-Bakry MY. Modeling of Transverse Momentum Spectra for Charged Particles in Proton-Proton Collisions Based on Soft Computing Approaches. *Journal of Computational and Theoretical Transport*. 2017;46:410-426. DOI: 10.1080/23324309.2017.1405272
- [6] Breiman L. Random Forests. *Machine Learning*. 2001;45:5-32. DOI: 10.1023/A:1010933404324
- [7] Ciresan D, Meier U, Masci J, Gambardella L, Schmidhuber J. Flexible, High Performance Convolutional Neural Networks for Image Classification. In: 22nd International Joint Conference on Artificial Intelligence, Barcelona, Catalona, Spain. July 16-22, 2011; pp. 1237-1242. DOI: 10.5591/978-1-57735-516-8/IJCAI11-210
- [8] Krizhevsky A, Sutskever I, Hinton G. *Proceedings of the Advances in Neural Information Processing Systems*. Vol. 25. NV, USA: Lake Tahoe; 2012. pp. 1090-1098
- [9] Ciresan D, Meier U, Schmidhuber J. Multi-Column Deep Neural Networks for Image Classification. In: *IEEE Conference on Computer Vision and Pattern Recognition*. 2012. pp. 3642-3649. DOI: 10.1109/CVPR.2012.6248110
- [10] Nauck D, Nürnberger A, Neuro-fuzzy Systems: A Short Historical Review A. *Studies in Computational Intelligence*. 2013;445:91-109. DOI: 10.1007/978-3-642-32378-2\_7
- [11] Mohd J, Abid H, Ravi PS, Rajiv S. Artificial Intelligence Applications for Industry 4.0: A Literature-Based Study. *Journal of Industrial Integration and Management*. 2022;07:83-111. DOI: 10.1142/S2424862221300040
- [12] Tiruneh GG, Fayek AR, Sumati V. Neuro-fuzzy systems in construction engineering and management research. *Automation in Construction*. 2020;119: 103348. DOI: 10.1016/j.autcon.2020.103348
- [13] El-Bakry SY, El-Bakry MY. Neural Network Representation For Electron and Positron Collisions with Sodium and Potassium. *Indian Journal of Physics*. 2004;78:1313-1318
- [14] Alaa FA, Habashy DA, Zahran HY, Soliman HN. Mathematical Modelling of Vickers Hardness of Sn-9Zn-Cu Solder Alloys Using an Artificial Neural Network. *Metals and Materials International*. 2021;27:4084-4096. DOI: 10.1007/s12540-020-00940-1
- [15] Alaa FA, Heba YZ, Habashy DA, Hana MA. Simulation and Prediction of



the Vickers Hardness of AZ91 Magnesium Alloy Using Artificial Neural Network Model, *Crystals*. 2020;**10**:290. DOI: 10.3390/cryst10040290

[16] Abd El-Rehim AF, Zahran HY, Al-Masoud HM, Habashy-DM. Microhardness and microstructure characteristics of AZ91 magnesium alloy under different cooling rate conditions, *Materials Research Express*. 2019;**6**: 086572-086587. DOI: 10.1088/2053-1591/ab1ad6

[17] Ali HAM, Habashy DM. The electrical impedance, AC conductivity and dielectric properties of phenol red compound investigated and modeled by an artificial neural network. *Communications in Theoretical Physics*. 2020;**72**:105701-105711. DOI: 10.1088/1572-9494/aba24d

[18] Habashy DM, El-Bakry-Mahmoud Y, Scheinast W, Hanafy M. Entropy per Rapidity in Pb-Pb Central Collisions using Thermal and Artificial Neural Network (ANN) Models at LHC Energies. *Chinese Physics C*. 2022;**46**:073103-073114. DOI: 10.1088/1674-1137/ac5f9d

[19] Habashy DM, El-Bakry Mahmoud Y, Tawfik A, Abdel Rahman RM, Hanafy M. Particles multiplicity based on rapidity in Landau and artificial neural network (ANN) models. *International Journal of Modern Physics A*. 2022;**37**: 2250002. DOI: 10.1142/S0217751X22500026

[20] Habashy DM, Mohamed HS, El-Zaidia EFM. A simulated neural system (ANNs) for micro-hardness of nano-crystalline titanium dioxide. *Physica B: Condensed Matter*. 2019;**556**:183-189. DOI: 10.1016/j.physb.2018.12.007

[21] Jang JSR. ANFIS: Adaptive-network-based fuzzy inference system. *IEEE Transactions on Systems, Man, and*

*Cybernetics: Systems*. 1993;**23**:665-684. DOI: 10.1109/21.256541

[22] Zadeh LA. Fuzzy sets. *Information and Control*. 1965;**8**:338-353. DOI: 10.1016/S0019-9958(65)90241-X

[23] Jang JSR, Sun CT. Neuro-fuzzy modeling and control. In: *Proceedings of the IEEE*. 1995;**83**:378-406

[24] Akkoyun S, Torun Y. Neuro-fuzzy modeling of deformation parameters for fusion-barriers. *Nuclear Engineering and Technology*. 2021;**53**:1612-1618. DOI: 10.1016/j.net.2020.10.017

[25] El-Bakry-M Y. A Study of K-P Interaction at High Energy using Adaptive Fuzzy Interface System. *International Journal of Modern Physics C (IJMPC)*. 2004;**15**:1013-1020. DOI: 10.1142/S0129183104006467

[26] ALICE Collaboration. Measurement of  $D^0$ ,  $D^+$ ,  $D^{*+}$  and  $D_s^+$  production in pp collisions at  $\sqrt{s} = 5.02$  TeV with ALICE. *European Physical Journal C: Particles and Fields*. 2019;**79**:388. DOI: 10.1140/epjc/s10052-019-6873-6

[27] ALICE Collaboration. Measurement of D-meson production at mid-rapidity in pp collisions at  $\sqrt{s} = 7$  TeV. *European Physical Journal C*. 2017;**77**:550. DOI: 10.1140/epjc/s10052-017-5090-4

[28] Khajeh A, Modarress H. Prediction of solubility of gases in polystyrene by Adaptive Neuro-Fuzzy Inference System and Radial Basis Function Neural Network. *Neural Network Expert Systems with Applications*. 2010;**37**: 3070-3074. DOI: 10.1016/j.eswa.2009.09.023

[29] Tortum A, Yayla N, Gökdağ M. The modeling of mode choices of intercity freight transportation with the artificial

*Artificial Intelligence Approaches for Studying the pp Interactions at...*  
DOI: <http://dx.doi.org/10.5772/intechopen.111552>

neural networks and adaptive neuro-fuzzy inference system. *Expert Systems with Applications*. 2009;**36**(3 Part 2): 6199-6217

[30] Behery GM, El -Harby AA, El -Bakry MY. ANFIS and Neural Networks Systems For Multiplicity Distributions in Proton-Proton Interactions. *Applied Artificial Intelligence*. 2013;**27**:304-322.  
DOI: 10.1080/08839514.2013.774212